HHS Public Access

Author manuscript

Org Chem Front. Author manuscript; available in PMC 2020 June 07.

Published in final edited form as:

Org Chem Front. 2019 June 7; 6(11): 1762–1774. doi:10.1039/C9QO00074G.

A joint molecular networking study of a *Smenospongia* sponge and a cyanobacterial bloom revealed new antiproliferative chlorinated polyketides

Roberta Teta[a], **Gerardo Della Sala**[b], **Germana Esposito**[a], **Christopher W. Via**[c], **Carmela Mazzoccoli**[b], **Claudia Piccoli**[b,d], **Matthew J. Bertin**[c], **Valeria Costantino**[a], **Alfonso Mangoni**[a]

[a.] Dipartimento di Farmacia, Università degli Studi di Napoli Federico II, via Domenico Montesano 49, 80131 Napoli, Italy

[b.] Laboratory of Pre-clinical and Translational Research, IRCCS-CROB, Referral Cancer Center of Basilicata, Via Padre Pio 1, 85028 Rionero in Vulture, Italy.

[c.] Department of Biomedical and Pharmaceutical Sciences, College of Pharmacy, University of Rhode Island, 7 Greenhouse Road, Kingston, RI 02881, United States

[d.] Department of Clinical and Experimental Medicine, University of Foggia, viale Pinto 1, 71122 Foggia, Italy.

Abstract

The bloom-forming cyanobacteria *Trichodesmium* sp. have been recently shown to produce some of the chlorinated peptides/polyketides previously isolated from the marine sponge *Smenospongia aurea*. A comparative analysis of extracts from *S. aurea* and *Trichodesmium* sp. was performed using tandem mass spectrometry-based molecular networking. The analysis, specifically targeted to chlorinated metabolites, showed that many of them are common to the two organisms, but also that some general differences exist between the two metabolomes. Following this analysis, six new chlorinated metabolites were isolated and their structures elucidated: four polyketides, smenolactones A-D (**1**-**4**) from *S. aurea*, and two new conulothiazole analogues, isoconulothiazole B (**5**) and conulothiazole C (**6**) from *Trichodesmium* sp. The absolute configuration of smenolactone C (**3**) was determined by taking advantage of the conformational rigidity of open 1,3-disubstituted alkyl chains. The antiproliferative activity of smenolactones was evaluated on three tumor cell lines, and they were active at low-micromolar or sub-micromolar concentrations.

Electronic Supplementary Information (ESI) available: Appendix A with demonstration of the relative configuration of C-5 and C-6/C-8 of smenolactone C (**3**). Appendix B with quantum mechanical prediction of ECD spectra of smenolactones A-D (**1**-**4**) and trichophycin B (**17**). Tables S1-S6 with detailed NMR data for compounds **1**-**6**. Table S7 with Cartesian coordinates of conformers of compound **1**. Figure S1 with the ECD spectra of reference chiral α,β-unsaturated δ-lactones and smenolactones A-D, Figure S2 with Marfey's analysis of compound **5,** and Figures S3–S36 with the 1D- and 2D-NMR and MS2 spectra of compounds **1**-**6**. See DOI: 10.1039/x0xx00000x

Conflicts of interest

There are no conflicts to declare

Introduction

The holobiome of marine sponges has proven to be an excellent source of lead compounds in, among others, anticancer,[1,2] immunomodulating,[3,4] and antibiotic[5,6] drug discovery. The term holobiome is used here to highlight that natural products from sponges (as well as those from many other organisms) are often the result of the biosynthetic architecture present in symbiotic microorganisms rather than in the cells of the host organisms.[7]

Sponges of the genus *Smenospongia* have recently been shown to contain a number of chlorinated mixed polyketide-peptides compounds. They include smenamides A (**7**) and B (**8**), active at nanomolar concentration on the Calu-1 lung cancer cell line,[8] smenothiazoles A (**9**) and B (**10**), cytotoxic at nanomolar levels through a pro-apoptotic mechanism with selectivity against ovarian cancer cells,[9] and conulothiazoles A (**11**) and B (**12**)[10] (Chart 2). Total synthesis unequivocally confirmed the structure of smenothiazoles[11] and smenamides, [12] and additionally determined the 16*R* configuration of smenamide A, unassigned in the original paper.

Besides being chlorinated, compounds **7**-**12** share a chlorovinylidene group that is characteristic of cyanobacterial metabolites such as jamaicamide[13] and the malyngamides. [14,15] This, together with the presence of other cyanobacterial structural motifs (such as the dolapyrrolidone ring of smenamides and the terminal alkyne of smenothiazole B) suggested a cyanobacterium associated with *S. aurea* to be the producer of compounds **7**-**12**.10

Very recently, analysis of a sample of the cyanobacterium *Trichodesmium* sp., collected in the Gulf of Mexico during a 2014 bloom event, revealed the presence of smenamides A (**7**) and B (**8**), smenothiazole A (**9**), three new smenamide analogs (smenamides C-E, **13**-**15**),[16] and trichophycins A-F (**16–21**),[17,18] new halogenated metabolites which are also clearly related to compounds **7**-**12** from *S. aurea* (Chart 2). Notably, four of the trichophycins are pure polyketides, rather than mixed polyketide-peptides like compounds **7**-**12.** Overall, these findings raise questions of how closely the metabolomes of *S. aurea* and *Trichodesmium* sp. are overlapped, and more specifically, whether *S. aurea* also contains chlorinated pure polyketides in addition to mixed polyketide-peptides.

In this paper, we report a comparative analysis of the organic extracts of *S. aurea* and *Trichodesmium* sp. The analysis was targeted to the chlorinated compounds present in the two organisms, and was performed combining high-resolution LC-MS/MS and molecular networking,[19] a recently-developed method for automated LC-MS data analysis and mining. The analysis showed that both *S. aurea* and *Trichodesmium* sp. contain a wide range of chlorinated compounds, that many of these compounds are present in both organisms, and that chlorinated pure polyketides are also present in *S. aurea*. Following this analysis, four new polyketides, smenolactones A-D (**1**-**4**) were isolated from *S. aurea*, and two new conulothiazole analogues, isoconulothiazole B (**5**) and conulothiazole C (**6**) were isolated from *Trichodesmium* sp., and their structures elucidated. Evaluation of the antiproliferative activity of smenolactones A, C and D and trichophycin B (**17**) is also described.

Results

Construction of molecular network

An extract of *S. aurea* enriched in chlorinated metabolites was prepared as described in our previous papers.[8–10] Shortly, a specimen of *S. aurea* was extracted with MeOH, and the extract partitioned between H_2O and BuOH; the sponge was then extracted in sequence with MeOH/$CHCl_3$ mixtures and with $CHCl_3$. All the organic extracts were combined and dried, and subjected to reversed-phase column chromatography using an RP-18 stationary phase. Finally, the fraction containing chlorinated metabolites was treated with acidic H_2O to remove brominated alkaloids, which are abundant in *S. aurea*, dried, and dissolved in MeOH at 1 mg/mL for LC-MS analysis. The crude extract of *Trichodesmium* sp. biomass was obtained as previously described17 by repeated extraction with 2:1 CH_2Cl_2:MeOH followed by concentration using reduced pressure to yield a crude extract.

The extracts from *S. aurea* and *Trichodesmium* were analyzed by liquid chromatography coupled with high-resolution electrospray mass spectrometry (LC-HR-ESI-MS) on an LTQ Orbitrap instrument. Data-dependent acquisition was used to trigger MS2 scans only for parent ions containing one chlorine atom (i.e. ions showing an M+2 isotope peak with a mass difference 1.9970±0.0010 and relative intensity 34±10%). The five most intense ions meeting the above requirements detected in each MS scan were fragmented in the subsequent MS2 scans. Before creating the molecular network, the raw LC-MS data were processed using the mzMine program[20] to distinguish between isomeric compounds (such as smenamide A and B) on the basis of their retention time, to remove isotopic peaks, and to perform quantitation (see Experimental section for details). The .mgf MS2 data file generated by mzMine was then submitted to the online platform at Global Natural Products Social Molecular Networking website (gnps.ucsd.edu),[21] and the network was visualized using the Cytoscape program.[22]

The resulting molecular network is shown in Figure 1. In the network, each node is represented as a pie chart showing the source of the compound (yellow: *S. aurea*, green: *Trichodesmium* sp.). It is apparent that there are many common metabolites between *S. aurea* and *Trichodesmium* sp., and most network clusters contain metabolites from both organisms. In particular, smenamide A (**7**), smenothiazole A (**9**) and B (**10**), and conulothiazole B (**11**), originally described from *S. aurea*, are also present in *Trichodesmium* sp.; conversely, trichophycins B (**17**) and F (**21**), originally described from *Trichodesmium* sp., are also present in *S. aurea*. It is to be noted that trichophycins C-E do not appear in the network because they contain two chlorine or one chlorine and one bromine atoms, and therefore they were not selected for MS2 fragmentation. Peaks corresponding to these compounds were sought manually in the LC-MS data from the extract of *S. aurea*, but they appeared not to be present.

We next focused our attention to the networks of non-nitrogenated polyketides. The network including trichophycin A only contained metabolites for *Trichodesmium* sp., but the network including trichophycin B clearly showed the presence in *S. aurea* (in addition to trichophycin B itself) of two isomers of trichophycin B and four additional analogues, all appearing to be new compounds. We were able to isolate five of these compounds in pure form, namely

trichophycin B (**17**) and four new chlorinated polyketides, which we called smenolactones A-D (**1**-**4**). Finally, the network including conulothiazoles A and B contained several new analogues, of which we could isolate in pure form two new conulothiazoles, isoconulothiazole B (**5**) and conulothiazole C (**6**).

Structure elucidation of smenolactones A-D

The molecular formula of smenolactone A (**1**) was determined as $C_{20}H_{24}ClO_3$ from the $[M+H]^+$ ion at *m*/*z* 347.1412 in the ESI mass spectrum, and confirmed by the $[M+Na]^+$ ion at *m*/*z* 369.1231 also present in the spectrum. In the proton NMR spectrum of **1** (Table 1, Table S1 in the Electronic Supplementary Information), the characteristic signal of the chlorovinylidene proton (δ 6.08, H-17) was clearly visible as a broad singlet at δ 6.08. The COSY spectrum showed H-17 to be allylically coupled with protons of two deshielded methylene groups, the benzylic methylene protons H_2-10 (in turn long-range coupled with the ortho aromatic protons), and the bis-allylic methylene protons H_2-8 (coupled with the olefinic proton H-7). Proton and carbon chemical shifts of this part of the molecule were very close to those of the corresponding atoms of smenothiazole A (**9**) that possesses an identical partial structure.9 The allylic couplings of H-7 with the methyl protons H_3-18 and the oxymethine proton H-5, and the homoallylic coupling of the methyl protons H_3-18 with the methylene protons H-4a and H-4b completed the carbon skeleton of **1**. The set of cross peaks detected in the HMBC spectrum (Figure 2A) was in full agreement with these structural assignments, and additionally located the methoxy group at C-3. Finally, the prominent ROESY correlation peak between H-17 and H_2-10 was used to assign the *E* configuration to the double bond at position 9, while those between H_3-18 and H_2-8 and between H-7 and H-5 were used to assign the *E* configuration to the double bond at position 6.

The absolute configuration at C-5, the only chiral center in **1**, was determined on the basis of the ECD spectrum, showing a negative Cotton effect at 255 nm (Δε −3.0). Compound **1** contains four separate chromophores, but the α,β-unsaturated δ-lactone is the only inherently chiral chromophore among them, and as such is expected to dominate the ECD spectrum. The ECD spectra of several chiral α,β-unsaturated δ-lactones structurally related with smenolactone A (**1**) are available in the literature, including (*S*)-7,8-dihydrokavain,[23] LL-P88Oα,[24] and coibacin A (in the latter compound, the carbinol of the α,β-unsaturated lactone is linked to a vinylic substituent as it is in **1**).[25] A clear correlation was found between the configuration of the lactone and the sign of the Cotton effect at 240–260 nm (Figure S1 in the Electronic Supplementary Information), supporting the *S* configuration at C-5 for **1**, i.e the opposite configuration compared to trichophycin B (**17**).

The $[M+H]^+$ ion at *m*/*z* 421.2136 in the ESI mass spectrum supported a molecular formula of $C_{24}H_{34}ClO_4$ for smenolactone B (**2**), which is therefore an isomer of trichophycin B (**17**). Analysis of the COSY, TOCSY, HSQC and HMBC 2D NMR spectra showed that compounds **2** and **17** share the same atom connectivity (Tables 1 and S2, Figure 2B) and are therefore stereoisomers. A clear difference between **2** and **17** was found in the configuration of the chlorovinylidene group, which was assigned as *Z* in **2** on account of the ROESY correlation peak of H-21 with H_2-14. In contrast, NMR parameters of the lactone end of **2**

were very close to those of **17**: ^{13}C NMR chemical shifts of carbons C-1 through C-10 and of the three methyl groups were identical, showing the relative configuration at C-5, C-6, C-8, and C-11 to be the same; the ^{1}H-^{1}H couplings of protons H-2 through H-8 were also very close (a precise measurement of the coupling constants of protons at C-9 and C-10 was not possible because of non-first-order multiplets). The ECD spectrum recorded for compound **2** was also very similar to that recorded for trichophycin B (**17**), showing the four chiral centers to have not only the same relative configuration, but also the same absolute configuration as in **17**. Therefore, structure of smenolactone B (**2**) was assigned as the geometric isomer at the chlorovinylidene of trichophycin B (**17**).

Smenolactone C (**3**) is a further stereoisomer of smenolactone B (**2**) and trichophycin B (**17**), and its planar structure, including the *Z* configuration of the chlorovinylidene group, was established much in the same way as described for **2** (Tables 1 and S3, Figure 2B). Therefore, smenolactone C (**3**) must be different from smenolactone B (**2**) in the configuration of one of more of the four chiral centers in the molecule. The 5*R* configuration was assigned (as discussed above for compound **2**, Figure S1) on the basis of the ECD spectrum of compound **3**, which was very similar to that of compounds **2** and **17**.

Relative configuration of C-6 and C-8 was determined on the basis of the following evidence. A systematic conformational study of branched alkanes[26] have shown that only two low-energy conformers of 2,4-dimethylpentane exist, because all the other conformers show at least one unfavorable *syn*-pentane interaction (similar to the unfavorable 1,3-diaxial interactions in a substituted cyclohexane, Figure 3A–C). This conformational behavior is common to any 1–3-disubstituted C_5 alkyl chain, including the C-5/C-9 segment of compound **3** (Figure 3D). Compound **3** shows a clear large/small coupling constant pattern for protons at C-7. Specifically, H-7b (δ 1.18) showed a large coupling (10.1 Hz) with H-6 and a small coupling (4.0 Hz) with H-8, while the opposite (3.7 and 10.3 Hz, respectively) was observed for H-7a (δ 1.36). This pattern clearly shows that the conformation on the right in Figure 3D is strongly preferred (the conformer on the left would have an opposite pattern), and therefore that the C-5/C-9 segment of compound **3** has a single conformation which is largely predominant. The presence of a rigid framework in the C-5/C-9 segment allows the use of NOESY data to assign relative configurations as it is usually done in cyclic compounds. Therefore, NOESY correlations of H_3-23 with H-8 and H-7b (but not with H-7a) and of H_3-22 with H-6 and H-7a (but not with H-7b) defined the *anti* orientation of the methyl groups CH_3-22 and CH_3-23 (Figure 3E), i.e. either the 6*R*,8*S* or the 6*S*,8*R* configuration (compound **2** has the 6*R*,8*R* configuration, with *syn* methyl groups).

The two possibilities were distinguished comparing the correlation peak between protons at C-4 and protons at C-7 observed in the NOESY spectrum with interatomic distances measured on the possible conformers of simplified models of 5*R*,6*R*,8*S*-**3** and 5*R*,6*S*,8*R*-**3** (see Appendix A in the Electronic Supplementary Information for a detailed discussion). Only the model of 5*R*,6*S*,8*R*-**3** could rationalize the observed NOESY correlation peaks. Configuration at C-11 was determined by examination of the ^{1}H NMR and ^{1}H-^{1}H COSY spectra of Mosher esters of **3**. Analysis of C-11 *R* and *S* MTPA esters showed negative $\Delta(\delta_H S-\delta_H R)$ values for H-14, H-21, and H-12 and positive values for H-9, H-8, H-22, and H-23 (Figure 4) supporting the 11*R* configuration as in compound **2**. Thus, the configuration

of smenolactone C (**3**) was assigned as 5*R*,6*S*,8*R*,11*R*, i.e. the C-6 epimer of smenolactone B (**2**).

Smenolactone D (**4**) showed a molecular formula $C_{24}H_{32}ClO_4$ based on the $[M+H]^+$ ion at *m*/*z* 419.1980 in the ESI mass spectrum, fitting a dehydro derivative of smenolactones B and C. Preliminary analysis of the ^1H NMR spectrum of **4** (Tables 1 and S4) showed that signals of the benzyl, chlorovinylidene and α,β-unsaturated lactone groups were all present in the spectrum, and showed chemical shifts and multiplicities similar to those of smenolactone B (**2**). However, one of the two methyl doublets of smenolactone B was replaced by a singlet at δ 1.61, and an additional signal for an olefinic proton (a triplet at δ 5.25) was present in the spectrum of **4.** The only possible location of an additional unsaturation on the skeleton of smenolactones B and C that fits these data was a double bond between C-8 and C-9. Analysis of the 2D NMR spectra (Figure 2C) confirmed this hypothesis. In particular, the homoallylic coupling between the methyl protons at δ 1.61 (H_3-22) and the methylene protons H_2-10 shown by COSY

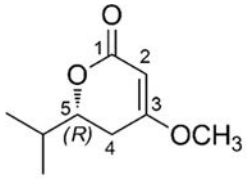

22

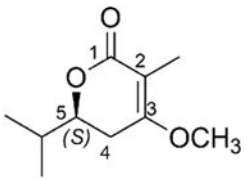

23

spectrum and the HMBC correlation between the same H_3-22 protons and C-7 unequivocally located the additional double bond of smenolactone D at position 8. The *E* configuration of this double bond was deduced from the ROESY correlation peaks of H_3-22 with H_2-10 and of H-7 with H-9. The configuration at C-6 could not be determined and was left unassigned, while the *S* configuration at C-5 was determined from the negative Cotton effect at 248 nm in the ECD spectrum (Figure S1). This is the same configuration as in smenolactone A (**1**), but different from that of smenolactones B (**2**) and C (**3**), and trichophycin B (**17**).

The different configuration of lactone ring between smenolactones prompted us to seek further support to our assignment in quantum mechanical calculation of ECD spectra (the calculations are described in detail in Appendix B, Electronic Supplementary Information). Preliminary calculations were performed using model compounds: compound **22** was chosen to study the isolated chiral lactone chromophore common to smenolactones B-D (**2**-**4**) and trichophycin B (**17**) (whose absolute configuration was also determined by empirical correlation of ECD spectra in the original paper),18 and compound **23** was chosen as a model for the chromophore of smenolactone A (**1**). The ECD spectra of compounds **22** and **23**, calculated at the B3LYP/6–31G(d,p) level of theory, were in full agreement with the empirical correlation described above. Subsequently, the possibility that the interaction with the other chromophores of the molecule could substantially affect the ECD spectra of compounds **1**-**4** and **17** in the region of interest was examined. To this purpose, the ECD spectra of the full molecules of trichophycin B (**17**) and smenolactone A (**1**) were calculated. The results (Figure 5 and Appendix B in the Electronic Supplementary Information) showed

that the empirically determined correlation between the configuration of the lactone and the sign of the Cotton effect at 240–260 nm was still valid, even in the presence of the additional chromophores present in the two molecules. Consequently, the absolute configuration of the lactone ring was confirmed as 5*S* for compounds **1** and **4**, and 5*R* for compounds **2**, **3**, and **17**.

Structure elucidation of isoconulothiazole B and conulothiazole C

Isoconulothiazole B (**5**) showed an $[M+H]^+$ ion at *m/z* 403.1603 supporting a molecular formula of $C_{22}H_{28}ClN_2OS$, identical to that of conulothiazole B (**12**). Preliminary examination of 1D and 2D NMR spectra (Table S5) supported the assignment of a thiazole residue, an alanine amino acid, and an extended polyketide chain. The only difference in the planar structures of **5** and **12** was the configuration of the chlorovinylidene moiety. NOE correlations between H-14 and H_2-12 and H-11a and H-11b supported the *Z* configuration of **5** and assigned it as the geometric isomer of **12**. The configuration at C-4 was determined by subjecting **5** to acid hydrolysis followed by a modified Marfey's method (L-FDVA as Marfey's reagent) utilizing *R* and *S* standards of 2-thiazolemethanamine similarly reacted with L-FDVA. Comparison of the reacted hydrolysate and the chromatographic standards (Figure S2) supported as 4*S* configuration identical to that of **12**. The configuration at C-10 is presently unassigned.

Additionally, we isolated a small amount of a related metabolite to **5**. Compound **6** showed an $[M+Na]^+$ ion at *m/z* 467.1913 supporting a molecular formula of $C_{25}H_{33}ClN_2OS$. The ^1H NMR spectrum indicated a molecule closely related to **5**. Examination of the MS/MS spectrum of **6** indicated that the modification was in the PKS portion of the molecule. A ^1H-^1H spin system was assigned, supported by COSY and TOCSY correlations placing an additional fully reduced propionate unit (H_2-9, H-10, and H_3-22) into the polyketide portion of **5** (Table S6), and characterizing the planar structure of conulothiazole C. The small amount of **6** isolated precluded further configuration analysis.

In vitro evaluation of antiproliferative activity of trichophycin B and smenolactones A, C, and D

In order to assess cell growth effects of trichophycin B and smenolactones A, C, and D, MCF-7 breast adenocarcinoma cells were initially tested at a single dose exposure (1 μM) and cell proliferation was evaluated by the MTS colorimetric assay, revealing a cytotoxic action exerted by these polyketides. In addition, microscopic observations showed an increased number of floating cells (indicative of cell death) in treated cells compared to untreated controls.

To get a deeper understanding of bioactivity of these compounds, the xCELLigence System Real-Time Cell Analyzer (RTCA) was used for monitoring proliferation of MCF7 cancer cells after drug exposure. This system allows real-time assessment of cell viability by measuring alterations of electronic impedance which reflect cell number and morphology. These alterations are converted into Cell Index (CI), which can be normalized at a given time point, to give the Normalized Cell Index (NCI).

All four compounds (**1**, **3**, **4**, and **17**) were tested individually on MCF7 cells at concentrations of 250 nM, 500 nM, 1 μM and 2 μM (Figure 6A) for 48 h. The real-time cell analysis showed that smenolactones (a) reduced cell viability and (b) increased tumor cell doubling time in a dose-dependent manner, thus suggesting an antiproliferative effect in this cell cancer type.

Notably, smenolactone C (**3**) and trichophycin B (**17**) proved to be the most active compounds, inducing a substantial NCI decrease at 1 μM and 2 μM, with the IC_{50} values predicted to be 918 nM and 652 nM, respectively. Moreover, at a concentration of 2 μM of trichophycin B (**17**), MCF-7 cells exhibited a drop in the NCI value below 0, corresponding to cell detachment, a consequence of cell death (Figure 6B). Growth inhibition was significantly less pronounced in MCF-7 cells treated with smenolactones A (**1**) and D (**4**), with the latter producing a significant effect only at the highest dose (2 μM).

For *in vitro* assessment of antiproliferative action selectivity, cytotoxic properties of smenolactones were also evaluated against PANC1 (pancreas ductal carcinoma) and BxPC-3 (pancreas adenocarcinoma) cell lines at 500 nM and 1 μM, within 48 h of treatment, by using the RTCA platform. PANC1 treated with smenolactones A (**1**) and D (**4**) experienced induced or unaffected proliferation at 500 nM and 1 μM, respectively, while BXPC-3 cell-growth was only slightly delayed at 1 μM concentration of each compound (Figure 7). Therefore, MCF7 cancer cells appear to be more sensitive to smenolactone A (**1**) than pancreatic cancer cell lines (Figure 8). On the other hand, treatment with 1 μM smenolactone C (**3**) and trichophycin B (**17**) produced a similar extent of toxicity in pancreas and breast cancer cells (Figures 7 and 8) indicating that these molecules exhibit an antiproliferative effect regardless the cell type at higher concentration. However, it is worthy to note that, unlike MCF-7 and BxPC-3 cells, PANC-1 cell proliferation appeared to be unaffected after treatment with 500 nM of smenolactone C (**3**) and trichophycin B (**17**) (Figure 7A).

Discussion

The results presented above clearly demonstrate the presence of a shared biosynthetic machinery in the free-living, bloom-forming cyanobacterium *Trichodesmium* sp. and in the holobiome of *S. aurea*. The three classes of chlorinated peptides/polyketides previously found in *S. aurea* (smenamides, smenothiazoles, and conulothiazoles) are all present in the extract of *Trichodesmium* sp., and, conversely, chlorinated polyketides related to trichophycin B are also present in *S. aurea*. However, some general differences were also found in the two metabolomes. The favored configuration of the chlorovinylidene appears to be different, as it can be seen comparing trichophycin B (**17**) and conulothiazole C (**6**) (more abundant or exclusively present in *Trichodesmium* sp.) with smenolactones A-D (**1–4**) or conulothiazole B (**12**) (more abundant or exclusively present in *S. aurea*). In addition, no compounds closely related with trichophycin A appear to be present in *S. aurea*.

An important open question is which organism hosts the biosynthetic genes of the polyketides and polyketide-peptides found in *S. aurea*, which have been found to be consistently present (albeit in low amounts) in all the specimens of *Smenospongia* we

analyzed. Because an increasing number of metabolites from sponges are produced by sponge-associated uncultivated bacteria,[27] the most obvious hypothesis was a cyanobacterium associated with *S. aurea*, and this was investigated in a previous study from our group.8 The composition of the cyanobacterial community in *S. aurea* was examined by PCR amplification of the metagenome of *S. aurea* with 16S primers specific for cyanobacteria. All the cyanobacterial sequences were identical at the 99% sequence identity threshold, and were assigned to Candidatus *Synechococcus spongiarum*. This is an uncultured unicellular sponge-specific symbiotic cyanobacterium, which is the most prevalent and widespread symbiotic cyanobacterium in tropical and temperate reef sponges. Since this study, the genomes of nine isolates of *S. spongiarum* from four sponge species have become available, and none of them contain PKS or NRPS gene clusters. Therefore, although horizontal gene transfer is not uncommon among cyanobacteria, in our opinion it is unlikely that *S. spongiarum* can host of such a variety of PKS and NRPS gene clusters. The new findings presented here suggest that the producer of the chlorinated metabolites found in *S. aurea* could be either a free living *Trichodesmium* species, indicating that the chlorinated compounds found in *S. aurea* would be dietary in origin, or a *Trichodesmium* species specifically associated with the sponge, but not so abundant as to be detected by the biomolecular methods used. Further studies will be necessary to confirm or disprove either hypothesis.

The present study is a further demonstration of the capacity of molecular networking to provide a quick and effective metabolic profiling of natural extracts, and to guide the discovery of new metabolites. Some methodological aspects that were used in this study, and were crucial to obtain a clear and informative molecular network, need to be stressed. First, an isotope peak filter was used in the selection of the precursor ions that would be subjected to MS2 fragmentation, and therefore would appear on the network. This selection needs to be made in real time during acquisition, because only a limited number of the ions detected in a full scan (in our case the five most intense ions) can be fragmented in the subsequent MS2 scans, and therefore fragmentation of non-target compounds (possibly co-eluting with the targets of the analysis) must be avoided. While the presence of a chlorine atom made selection based on isotope peaks particularly easy, different filters can be imagined (for example filters related to the excess of mass to select highly unsaturated compounds), the main limitation being the capabilities of the spectrometer software. Secondly, preprocessing of data using mzMine allowed the incorporation of LC data in the network in an automated way. This was essential for identification of the many isomeric compounds present in the extracts, and in particular of the new polyketides smenolactones C (**3**) and D (**4**), which are stereoisomers of trichophycin B (**17**). These metabolites show very similar MS2 spectra, and can only be distinguished by their HPLC retention times. Finally, it is interesting to note that smenothiazoles (**9** and **10**) were correctly shown to be present in both extracts, but appeared as isolated nodes in the network, in spite of their close structural correlation to each other. The reason for this was clear when their MS2 spectra were examined: both spectra contained a single, very intense, fragment ion at m/z 155.06, corresponding to the very stable 2-(2-thiazolyl)pyrrolidinium ion deriving from the cleavage of the amide bond of **9** and **10**. Compounds that, like smenothiazoles, produce only one or two fragment ions in their MS2 spectra are undoubtedly a problem for MS-based molecular networking, which requires at

least a few matched fragment peaks (the minimum number can be set, the default value is 6) to connect two nodes.

The chlorinated polyketides **1**, **3**, **4**, and **17** were assayed for their antiproliferative activity on three tumor cell lines, and were all active at low-micromolar or sub-micromolar concentrations. Although preliminary, the results have also highlighted some trends for bioactivity:

1. The polyketide chain length and flexibility affect antiproliferative activity: smenolactone C (**3**) and trichophycin B (**17**), that have a longer carbon chain and no double bonds, are the most bioactive compounds.
2. The *R* configuration at C-5 of the lactone moiety may be crucial to keep a strong bioactivity profile: smenolactones A (**1**) and D (**4**), with *S* stereochemistry at C-5, showed weaker cell growth inhibition.
3. The configuration of chlorovinylidene does not affect dramatically the antiproliferative effect because smenolactone C (**3**) and trichophycin B (**17**) displayed similar growth-inhibitory properties in the tested cell lines.

The chlorinated polyketides from *S. aurea* are part of an increasing group of potential antitumor lead compounds from *Smenospongia* species.[8,9] The preliminary results reported here will be the basis for a deeper study of the biological activity of these compounds, which in addition will be extended to the other analogues that are in our hands or will be isolated in the future.

Experimental

General methods

Optical rotations were measured using a Jasco P-200 polarimeter. UV spectra were measured using a Beckman Coulter DU-800 spectrophotometer. ECD spectra were recorded on a Jasco J-715 spectrophotometer using a 1-mm cell. NMR spectra were determined on Varian Unity Inova spectrometers at 700 MHz; chemical shifts were referenced to the residual solvent signal (CD_3OD: δ_H 3.31, δ_C 49.00). Other NMR data were recorded using a Bruker 800 MHz NMR and a Varian 500 MHz NMR; chemical shifts were referenced to the residual solvent signal (DMSO-d_6: δ_H 2.51, δ_C 39.5). For an accurate measurement of the coupling constants, the one-dimensional ^{1}H NMR spectra were transformed at 64 K points (digital resolution: 0.09 Hz). Through-space ^{1}H connectivities were evidenced using a ROESY or NOESY experiment with a mixing time of 450 ms. The HSQC spectra were optimized for $^1J_{CH}$ = 142 Hz, and the HMBC experiments for $^{2,3}J_{CH}$ = 8.3 Hz. HRESIMS analysis of the new conulothiazoles was performed using an AB SCIEX TripleTOF 4600 mass spectrometer with Analyst TF software. High performance liquid chromatography (HPLC) separations were achieved on an Agilent 1260 Infinity Quaternary LC apparatus equipped with a Diode-Array Detector (DAD). The new conulothiazoles were isolated using a Dionex UltiMate 3000 HPLC system each equipped with a micro vacuum degasser, an autosampler, and a DAD.

Collection, extraction, and isolation

A sample of *Smenospongia aurea* was collected at 12 m depth by Scuba along the coast of Mayaguana Island, Bahamas (GPS 22 27.0743N, 073 07.9688W) during the 2013 Pawlik expedition. The specimen (reference number 36713) was frozen immediately after collection and stored at −20 °C until extraction. The sponge (520.0 g wet weight) was homogenized and extracted with MeOH (4 × 4L), MeOH and $CHCl_3$ in different ratios (2:1, 1:1, 1:2) and then with $CHCl_3$ (2 × 4L). The MeOH extracts were partitioned between H_2O and n-BuOH; the BuOH layer was combined with the $CHCl_3$ extracts and concentrated in vacuo.

The organic extract (7.60 g) was chromatographed on a column packed with RP-18 silica gel. The fraction eluted with MeOH/H_2O (8:2, 396.3 mg) was partitioned in a two-phase system composed of H_2O (160 mL), MeOH (260 mL), $CHCl_3$ (140 mL), and AcOH (5 mL); the organic layer, containing smenothiazoles, smenamides and smenolactones, was subjected to reversed-phase HPLC separation [column 250 × 10 mm, 10 μm, Luna (Phenomenex) C18; eluent A: H_2O; eluent B: MeOH; gradient: 55→100% B, over 60 min, flow rate 5 mLmin $^{-1}$], thus affording five fractions, each containing one of compounds **1–4** and **17**. These fractions were individually purified on reversed-phase HPLC [column 250 × 4.6 mm, 5 μm, Luna (Phenomenex) C18; eluent A: H_2O; eluent B: ACN; gradient: 50→100% B, over 35 min, flow rate 1 mL min^{-1}], which gave smenolactone A (**1**) (165 μg, t_R = 21.0 min), smenolactone B (**2**) (202 μg, t_R = 21.0 min), smenolactone C (**3**) (182 μg, t_R = 21.4 min), smenolactone D (**4**) (93 μg, t_R = 18.2 min), and trichophycin B (**17**) (211 μg, t_R = 21.2 min).

The extract (3.95 g) and the VLC chromatography fractions of *Trichodesmium* biomass were prepared as previously described generating nine fractions from the initial extract.17 Three fractions (E: 40% hexanes in EtOAc; F: 20% hexanes in EtOAC; and I: 100% MeOH) were further processed. *F*ractions E and F were combined and subjected to C18 SPE fractionation using an elution scheme of 50% ACN in water, 100% ACN, 100% MeOH, and 100% EtOAC. Fraction I was subjected to the same procedure. The 100% ACN fraction of E and F was subjected to RP-HPLC using a YMC ODS column [250 × 4.6 mm, 5 μm] and a flow rate of 3 mLmin^{-1}. The solvent system was 40% water in ACN with each solvent modified with 0.5% formic acid, which gave isoconulothiazole B (**5**) (0.5 mg, t_R = 17.5 min). The 100% ACN fraction of I was also subjected to RP-HPLC using the same YMC column and a solvent system of 25% water in ACN with 0.5% formic acid in each solvent and a flow rate of 3 mL min^{-1}, which gave conulothiazole C (**6**) (t_R = 20.5 min).

Smenolactone A (1): colorless oil; UV (ACN): λ_{max} (ε) 244 (9700); ECD (ACN): λ_{max} (Δε) 255 (−3.0), 210 (–2.0); HRESIMS *m/z* 347.1407, $[M+H]^+$ (calcd for $C_{20}H_{24}ClO_3^+$, 347.1408, Δ –0.5 ppm); ^1H and ^{13}C NMR (CD_3OD): Table 1 and S1.

Smenolactone B (2): colorless oil; UV (ACN): λ_{max} (ε) 233 (13000); ECD (ACN): λ_{max} (Δε) 248 (+16.2); HRESIMS *m/z* 421.2136, $[M+H]^+$ (calcd for $C_{24}H_{34}ClO_4^+$, 421.2140, Δ –1.0 ppm); ^1H and ^{13}C NMR (CD_3OD): Tables 1 and S2.

Smenolactone C (3): colorless oil; UV (ACN): λ_{max} (ε) 234 (14700); ECD (ACN): λ_{max} (Δε) 246 (+10.2), 219 (–5.4); HRESIMS *m/z* 421.2136, $[M+H]^+$ (calcd for $C_{24}H_{34}ClO_4^+$, 421.2140, Δ –1.0 ppm); ^1H and ^{13}C NMR (CD_3OD): Tables 1 and S3.

Smenolactone D (4): colorless oil; UV (ACN): λ_{max} (ε) 232 (13500); ECD (ACN): λ_{max} (Δε) 248 (–12.8); HRESIMS (positive ion mode, MeOH) *m/z* 419.1980, $[M+H]^+$ (calcd for $C_{24}H_{32}ClO_4^+$, 419.1984, Δ –1.0 ppm); ^1H and ^{13}C NMR (CD_3OD), see Tables 1 and S4.

Isoconulothiazole B (5): colorless oil; $[\alpha^{23}_D]$ +4.5 (*c* 0.05, MeOH) UV (MeOH) λ_{max} (ε) 203 (3126), 235 (2590) nm; HRESIMS *m/z* 403.1603 $[M+H]^+$ (calcd for $C_{22}H_{28}ClN_2OS^+$, 403.1605, Δ –0.6 ppm); ^1H and ^{13}C NMR (DMSO-d_6), Table S5.

Conulothiazole C (6): colorless oil; UV (from UV scan during HPLC isolation): 209, 242 nm; HRESIMS *m/z* 467.1913 $[M+Na]^+$ (calcd for $C_{25}H_{33}ClN_2OSNa^+$, 467.1894, Δ +4.0 ppm); ^1H NMR (DMSO-d_6), Table S6.

Isotope-filtered data-dependent LC-HRMS/MS analysis

Experiments were performed using a Thermo LTQ Orbitrap XL high-resolution ESI mass spectrometer coupled to Thermo U3000 HPLC system, which included a solvent reservoir, in-line degasser, binary pump and refrigerated autosampler. A 5-μm Kinetex C18 column (50 × 2.10 mm), maintained at room temperature, was eluted at 200 $\mu L \cdot min^{-1}$ with H_2O (supplemented with 0.1% HCOOH) and MeOH, using a gradient elution. The gradient program was as follows: 45% MeOH 1 min, 45%–80% MeOH over 30 min, 100% MeOH 9 min. Mass spectra were acquired in positive ion detection mode. MS parameters were a spray voltage of 4.8 kV, a capillary temperature of 285 °C, a sheath gas rate of 32 units N_2 (ca. 150 mL/min), and an auxiliary gas rate of 15 units N_2 (ca. 50 mL/min). Data were collected in the isotope-filtered data-dependent acquisition mode, in which only ions containing one chlorine atom are selected for fragmentation based on the characteristic $^{37}Cl/^{35}Cl$ mass difference and intensity ratio. Specifically, only the first, the second until the fifth most intense ions of a full-scan mass spectrum showing an M+2 isotope peak with a mass difference 1.9970±0.0010 and relative intensity 34±10% were subjected to high resolution tandem mass spectrometry (HRMS/MS) analysis. HRMS/MS scans were obtained for selected ions with CID fragmentation, isolation width of 3.0, normalized collision energy of 35, Activation Q of 0.250, and activation time of 30 ms.

MZmine processing

LC-HRMS/MS raw files were directly imported into MZmine 2.23.20 Raw data files were filtered by cropping retention times range to 16–40 min and *m/z* range to 0–600 amu. The mass detection was performed on centroided data and exact masses with mass level 1, by keeping the noise level at 0. FTMS shoulder peaks were removed according to Lorentzian peak model, at resolution of 60000. Chromatograms were built using a minimum time span of 0.20 min, minimum height of 100000, and *m/z* tolerance of 0.01 (or 20 ppm). For the chromatogram deconvolution, the local minimum search algorithm was used with the following settings: chromatographic threshold = 10%, minimum retention time range = 0.20 min, minimum relative height = 30%, minimum absolute height = 100000, minimum ratio of peak top/edge = 1.3, peak duration range = 0.0−6.0 min. Peak alignment was performed using the Join aligner algorithm (*m/z* tolerance at 0.002 (or 10 ppm), absolute RT tolerance 0.3 min). $[M-^{37}Cl+^{35}Cl]$ ions were identified and extracted through Adduct search by RT tolerance of 0.1 min, *m/z* tolerance of 0.002 (or 10 ppm), and a maximum relative height of

400%; [M+Na–H], [M+K–H], [M+Mg–2H], [M+NH_3], [M-Na+NH_4], [M+1, ^{13}C] adducts were filtered out by setting the maximum relative height at 100%. Peaks without associated MS/MS spectrum were finally filtered out from peak list. Clustered data were then exported to .mgf file for GNPS.

Molecular networking

A molecular network21 was created using the online workflow at GNPS (https://gnps.ucsd.edu/). The parent mass tolerance and MS/MS fragment ion tolerance were both set at 0.02 Da. A network was then created where edges were filtered to have a cosine score above 0.6 and more than 6 matched peaks. Further edges between two nodes were kept in the network if each of the nodes appeared in each other's respective top 20 most similar nodes. The spectra in the network were then searched against GNPS spectral libraries. All matches kept between network spectra and library spectra were required to have a score above 0.7 and at least 6 matched peaks. Once the basic molecular network had been generated, the network was loaded into Cytoscape 3.2.122 and the Enhanced Graphics plug-in[28] was used to quantify and visualize outputs data with pie charts.

Marfey's analysis

Marfey's Amino Acid Standards.—A 50 mM solution of each amino acid standard, (*S*)-1-(1,3-thiazol-2-yl)ethanamine purchased from Enamine and (*R*)-1-(Thiazol-2-yl)ethanamine purchased from 1 Click Chemistry was created. 50 μL of each were placed in separate 2 mL vials. 100 μL of FDVA solution (10 mg/mL in acetone) was added to each vial followed by 20 μL of 1 M $NaHCO_3$ and 10 μL of DMSO. Each vial was placed capped and parafilmed into a sand bath stirring at 40 ^{o}C for 1 h. After 1 hour, the reactions were cooled and quenched with 20 μL of 1 M HCl. Then dried under N_2 for about one hour. After drying, 1 mL of 50:50 MeOH:H_2O was added to each and the standards were filtered and subjected to HPLC analysis.

Hydrolysis and Marfey's reactions of isoconulothiazole.—0.2 mg of **5** was dissolved in 500 μL of 6 N HCl and placed in a silicone oil bath at 100 °C stirring for 15 hours. After 15 hours, it was dried under N_2 for 1 hour, then 300 μL of $NaHCO_3$ was added along with 50 μL of FDVA (10 mg/mL in acetone) and 10 μL of DMSO. This was placed in a sand bath at 40 °C, stirring for 1 hour. After 1 hour the reaction was quenched with 100 μL of 1 M HCl, diluted with 200 μL of ACN and subjected to HPLC analysis. The hydrolysate and standards were subjected to RP-HPLC using a Kinetex C18 (Phenomenex) 150 × 4.6 mm, 2.6 μm column. The flow rate was set at 0.6 mLmin^{-1} and the initial conditions were set at 80% water and 20% ACN with 0.5% formic acid in each solvent. A linear gradient was employed for 80 min to a ratio of 50:50 water and ACN. Initial conditions were restored from min 81 to 90. The hydrolysate and the *S* standard both eluted at 54.10 min while the *R* standard eluted 48.25 min.

Generation of Mosher esters

0.4 mg of **3** was dissolved in dry $CDCl_3$ and separated into two equal portions in 4 mL vials. Dry pyridine (10 μL) and (*S*)-(+)-α-methoxy-α-(trifluoromethyl)phenylacetyl chloride (10 μL) were added to the first vial. The vial was capped, and the reaction mixture was stirred

for 24 h. The identical procedure was repeated with an equal amount of **3** and (*R*)-(−)-α-methoxy-α-(trifluoromethyl)phenylacetyl chloride. These reactions yielded the C-11 *R* ester from (*S*)-MTPA-Cl and the C-11 *S* ester from (*R*)-MTPA-Cl. After 24 h, the contents of the vials were immediately transferred to NMR tubes and ^{1}H NMR and ^{1}H-^{1}H COSY spectra were recorded.

Cell culture

MCF7, PANC-1 and BxPC-3 cells were purchased from American Type Culture Collection (ATCC, Manassas, VA, Usa). MCF7 cells were cultured in DMEM medium, while PANC-1 and BxPC-3 cells in RPMI medium, at 37°C in a 5% CO_2 humidified atmosphere. DMEM and RPMI media were supplemented with 10% fetal bovine serum, penicillin–streptomycin (100 U/ml), and 2 mM L-glutamine. Cell morphology was observed at inverted optical microscope (Axio Vert A1, Zeiss). When cells reached the confluence, cells were detached with 0.05% trypsin-EDTA to perform xCELLIgence assays.

xCELLigence assay

The xCELLigence System Real-Time Cell Analyzer (ACEA Biosciences) was used for monitoring proliferation of cancer cells. In our assays, 100 μL of media were added to each well of the 16-well E-plates to measure impedance background values. Then, 100 μL of cell suspension was added to reach a cell density of 3000 cells/well for MCF7 cells and a cell density of 2500 cells/well for PANC1 and BxPC-3 cells. Cells were keptd at RT for 30 minutes, and then the E plates were connected to the RTCA system placed into a cell incubator at 37°C and 5% CO_2. When cells reached log growth phase approximately 24 h later from seeding, medium was removed, and cells were treated with 200 μL of medium containing determined concentrations of each compound for 48 hours. Negative controls were treated with DMSO vehicle (0.5% final concentration). Cell proliferation was monitored every 30 min for a period of up to 72 h, measuring electrical impedance as a dimensionless parameter termed cell index (CI), by the RTCA-integrated software. After seeding cells, CI values increased. The increase of CI correlates with the increase in attached cell number. All experiments were performed in triplicate.

Statistical analysis

In our assays, CI was normalized just after drug treatment and converted into normalized cell index (NCI). Normalized cell index is calculated as follows: $NCI = CI_{\text{end of treatment}}/CI_{\text{normalization time}}$. Real-time NCI traces (e.g. Figure 6B) were obtained by the RTCA-integrated software. Antiproliferative effects of smenolactones and trichophycin B are presented either as NCI relative to controls treated with DMSO vehicle or as cell doubling time. Doubling time is the time required for a curve cell index value to double and was calculated by the RTCA-integrated software. Data are presented as mean ± standard deviation (n=3). Differences between groups were determined by analysis of variance (ANOVA) to determine statistical significance which is reported as *p* value. Statistical analysis was performed using the GraphPad Prism Software Version 5.

Dose-response curves for smenolactone C (r^2=0.9598) and trichophycin B (r^2= 0.9819) against MCF7 cancer cells were calculated using (a) NCI values at four different

concentrations (250 nM, 500 nM, 1 μM, 2 μM) and (b) the variable slope sigmoid equation to predict IC_{50} values. Smenolactone C (**3**) has an IC_{50} of 917,8 ± 115.8 nM (±SE), while trichophycin B (**17**) has an IC_{50} of 652 ± 56.9 nM (±SE). Dose-response curves and IC_{50} values were calculated using the GraphPad Prism Software Version 5.

Supplementary Material

Refer to Web version on PubMed Central for supplementary material.

Acknowledgements

This research was partially funded by Regione Campania, POR Campania FESR 2014–2020, O.S. 1.2, Project “Campania Oncoterapie”, grant no. B61G18000470007. Sponge collection was made possible by UNOLS funding through a grant from the US-NSF Biological Oceanography Programme (OCE 1029515) and the crew of the R/V Walton Smith (University of Miami). Warm thanks are due to Sven Zea (Universidad Nacional de Colombia) for confirming the identification aboard the ship. Some research reported in this publication was made possible by the use of spectrometric and spectroscopic equipment and services available through the RIINBRE Centralized Research Core Facility, which is supported by the Institutional Development Award (IDeA) Network for Biomedical Research Excellence from the National Institute of General Medical Sciences of the National Institutes of Health under Grant P20GM103430. Some NMR spectra were performed at the “Laboratorio di Tecniche Spettroscopiche”, Dipartimento di Farmacia, Università di Napoli Federico II; the assistance of Dr. Paolo Luciano is gratefully acknowledged. Certain NMR experiments were conducted at a research facility at the University of Rhode Island supported in part by the National Science Foundation EPSCoR Cooperative Agreement #EPS-1004057. This work was supported in part by an American Society of Pharmacognosy Starter Grant awarded to MB.

Notes and references

1. Hu Y, Chen J, Hu G, Yu J, Zhu X, Lin Y, Chen S and Yuan J, Mar. Drugs, 2015, 13, 202–221. [PubMed: 25574736]
2. Esposito G, Bourguet-Kondracki M-L, Mai LH, Longeon A, Teta R, Meijer L, Van Soest R, Mangoni A and Costantino V, J. Nat. Prod, 2016, 79, 2953–2960. [PubMed: 27933894]
3. Costantino V, Fattorusso E, Imperatore C and Mangoni A, European J. Org. Chem, 2003, 1433–1437.
4. Costantino V, Fattorusso E, Imperatore C, Mangoni A and Teta R, European J. Org. Chem, 2009, 2112–2119.
5. Saurav K, Bar-Shalom R, Haber M, Burgsdorf I, Oliviero G, Costantino V, Morgenstern D and Steindler L, Front. Microbiol, 2016, 7, 416. [PubMed: 27092109]
6. Costantino V, Della Sala G, Saurav K, Teta R, Bar-Shalom R, Mangoni A and Steindler L, Mar. Drugs, 2017, 15, 59.
7. Wilson MC and Piel J, Chem. Biol, 2013, 20, 636–647. [PubMed: 23706630]
8. Teta R, Irollo E, Della Sala G, Pirozzi G, Mangoni A and Costantino V, Mar. Drugs, 2013, 11, 4451–4463. [PubMed: 24217287]
9. Esposito G, Teta R, Miceli R, Ceccarelli LS, Della Sala G, Camerlingo R, Irollo E, Mangoni A, Pirozzi G and Costantino V, Mar. Drugs, 2015, 13, 444–459. [PubMed: 25603342]
10. Esposito G, Della Sala G, Teta R, Caso A, Bourguet-Kondracki ML, Pawlik JR, Mangoni A and Costantino V, European J. Org. Chem, 2016, 2016, 2871–2875.
11. Ma X, Chen Y, Chen S, Xu Z and Ye T, Org. Biomol. Chem, 2017, 15, 7196–7203. [PubMed: 28813067]
12. Caso A, Mangoni A, Piccialli G, Costantino V and Piccialli V, ACS Omega, 2017, 2, 1477–1488. [PubMed: 30023636]
13. Edwards DJ, Marquez BL, Nogle LM, McPhail K, Goeger DE, Roberts MA and Gerwick WH, Chem. Biol, 2004, 11, 817–833. [PubMed: 15217615]
14. Wu M, Milligan KE and Gerwick WH, Tetrahedron, 1997, 53, 15983–15990.

15. Kwan JC, Teplitski M, Gunasekera SP, Paul VJ and Luesch H, J. Nat. Prod, 2010, 73, 463–466. [PubMed: 20166701]
16. Via CW, Glukhov E, Costa S, Zimba PV, Moeller PDR, Gerwick WH and Bertin MJ, Front. Chem, 2018, 6, 1–9. [PubMed: 29441345]
17. Bertin M, Wahome P, Zimba P, He H and Moeller P, Mar. Drugs, 2017, 15, 10.
18. Bertin MJ, Saurí J, Liu Y, Via CW, Roduit AF and Williamson RT, J. Org. Chem, 2018, 83, 13256–13266. [PubMed: 30280904]
19. Teta R, Della Sala G, Glukhov E, Gerwick L, Gerwick WH, Mangoni A and Costantino V, Environ. Sci. Technol, 2015, 49, 14301–14310. [PubMed: 26567695]
20. Pluskal T, Castillo S, Villar-Briones A and Orešič M, BMC Bioinformatics, 2010, 11, 395. [PubMed: 20650010]
21. Wang M, Carver JJ, Phelan VV, Sanchez LM, Garg N, Peng Y, Nguyen D-TDD, Watrous J, Kapono CA, Luzzatto-Knaan T, Porto C, Bouslimani A, V Melnik A, Meehan MJ, Liu W-T, Crüsemann M, Boudreau PD, Esquenazi E, Sandoval-Calderón M, Kersten RD, Pace LA, Quinn RA, Duncan KR, Hsu C-C, Floros DJ, Gavilan RG, Kleigrewe K, Northen T, Dutton RJ, Parrot D, Carlson EE, Aigle B, Michelsen CF, Jelsbak L, Sohlenkamp C, Pevzner P, Edlund A, McLean J, Piel J, Murphy BT, Gerwick L, Liaw C-C, Yang Y-L, Humpf H-U, Maansson M, Keyzers RA, Sims AC, Johnson AR, Sidebottom AM, Sedio BE, Klitgaard A, Larson CB, Boya PCA, Torres-Mendoza D, Gonzalez DJ, Silva DB, Marques LM, Demarque DP, Pociute E, O'Neill EC, Briand E, Helfrich EJN, Granatosky EA, Glukhov E, Ryffel F, Houson H, Mohimani H, Kharbush JJ, Zeng Y, Vorholt JA, Kurita KL, Charusanti P, McPhail KL, Nielsen KF, Vuong L, Elfeki M, Traxler MF, Engene N, Koyama N, Vining OB, Baric R, Silva RR, Mascuch SJ, Tomasi S, Jenkins S, Macherla V, Hoffman T, Agarwal V, Williams PG, Dai J, Neupane R, Gurr J, Rodríguez AMC, Lamsa A, Zhang C, Dorrestein K, Duggan BM, Almaliti J, Allard P-M, Phapale P, Nothias L-F, Alexandrov T, Litaudon M, Wolfender J-L, Kyle JE, Metz TO, Peryea T, Nguyen D-TDD, VanLeer D, Shinn P, Jadhav A, Müller R, Waters KM, Shi W, Liu X, Zhang L, Knight R, Jensen PR, Palsson BØ, Pogliano K, Linington RG, Gutiérrez M, Lopes NP, Gerwick WH, Moore BS, Dorrestein PC and Bandeira N, Nat. Biotechnol, 2016, 34, 828–837. [PubMed: 27504778]
22. Shannon P, Markiel A, Ozier O, Baliga NS, Wang JT, Ramage D, Amin N, Schwikowski B and Ideker T, Genome Res, 2003, 13, 2498–2504. [PubMed: 14597658]
23. Pescitelli G, Bilia AR, Bergonzi MC, Vincieri FF and Di Bari L, J. Pharm. Biomed. Anal, 2010, 52, 479–483 [PubMed: 20185265]
24. Ellestad GA, McGahren WJ and Kunstmann MP, J. Org. Chem, 1972, 37, 2045–2047. [PubMed: 5037459]
25. Carneiro VMT, Avila CM, Balunas MJ, Gerwick WH and Pilli RA, J. Org. Chem, 2014, 79, 630–642. [PubMed: 24359482]
26. Hoffmann RW, Stahl M, Schopfer U and Frenking G, Chem. - A Eur. J, 1998, 4, 559–566.
27. Moosmann P, Ueoka R, Grauso L, Mangoni A, Morinaka BI, Gugger M and Piel J, Angew. Chemie Int. Ed, 2017, 56, 4987–4990.
28. Morris JH, Kuchinsky A, Ferrin TE and Pico AR, F1000Research, 2014, 3, 147. [PubMed: 25285206]

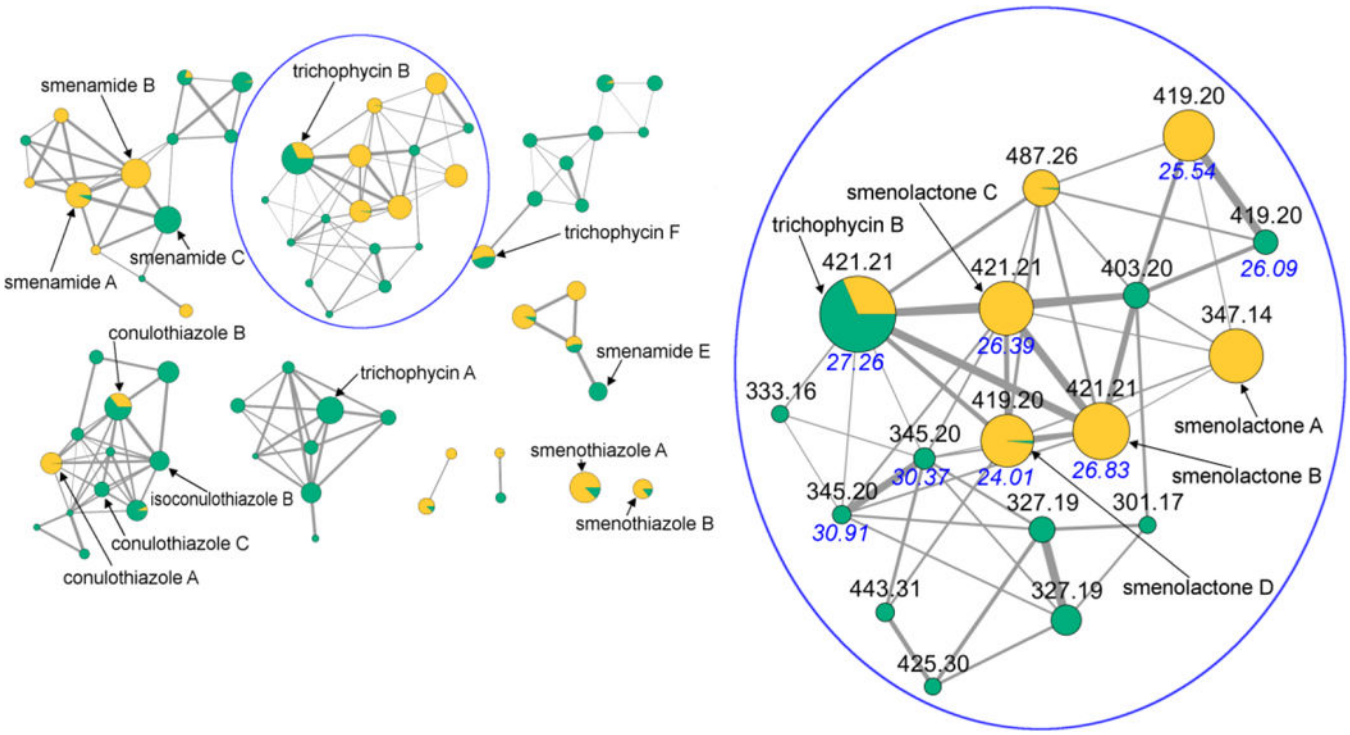

Fig. 1.

The molecular network obtained combining the LC-MS/MS analyses of extracts from *S. aurea* and *Trichodesmium sp.*. Nodes are represented as a pie chart showing the source of the compound (yellow: *S. aurea*, green: *Trichodesmium* sp.). Node size is relative to ion count, edge thickness is relative to cosine score. The networking cluster containing trichophycin B (**17**) and the new smenolactones A-D (**1**-**4**) is expanded, and nodes are labeled with parent *m*/*z* values and HPLC retention times. Retention times of isomeric compounds are shown in blue.

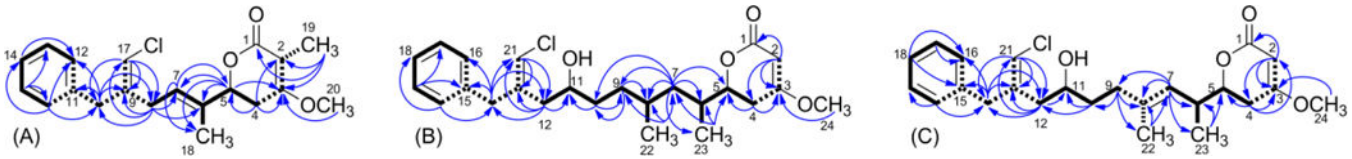

Fig. 2.

Key connections determined from 2D NMR spectra for compound **1** (A), compounds **2** and **3** (B) and compound **4** (C). Bold bonds are used to show proton-proton connections determined through vicinal couplings, dashed bold bonds are used to show proton-proton connections determined through allylic and homoallylic couplings, and arrows are used to show HMBC correlations.

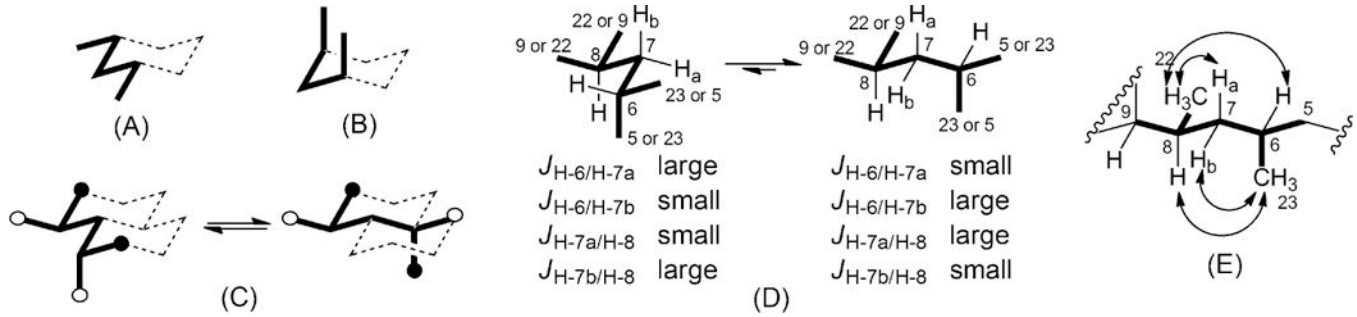

Fig. 3.

(A) The most stable conformer of pentane. (B) A high-energy conformer of pentane showing the destabilizing *syn*-pentane interaction. (C) The two only low-energy conformers of 2,4-dimethylpentane. (D) The two only possible low-energy conformations of the C-5/C-9 segment of compound **3**. Coupling constants of H-7a and H-7b show that the conformation shown on the right is highly preferred, whatever configurations at C-6 and C-8 may be. (E) NOESY correlations of H_3-23 with H-8 and H-7b (but not with H-7a) and of H_3-22 with H-6 and H-7a (but not with H-7b) define relative configuration of C-6 and C-8.

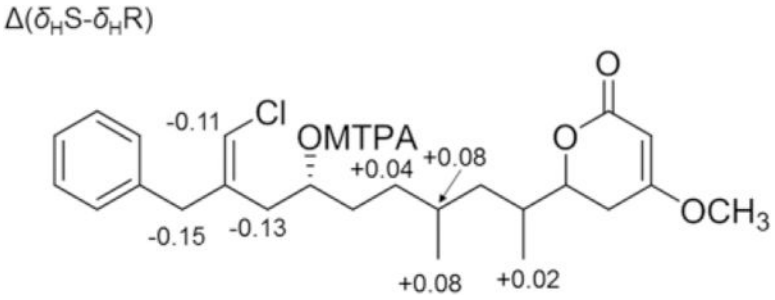

Fig. 4.

Δ($\delta_H S$-$\delta_H R$) values determined for *S*- and *R*-MTPA esters of smenolactone C (**3**).

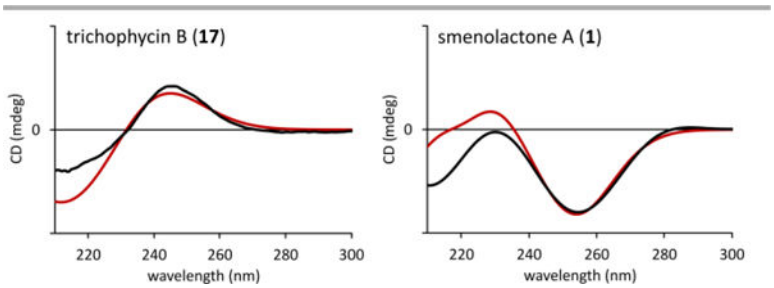

Figure 5.

Predicted (red curve) and experimental (black curve) ECD spectra of trichophycin B (**17**) and smenolactone A (**1**).

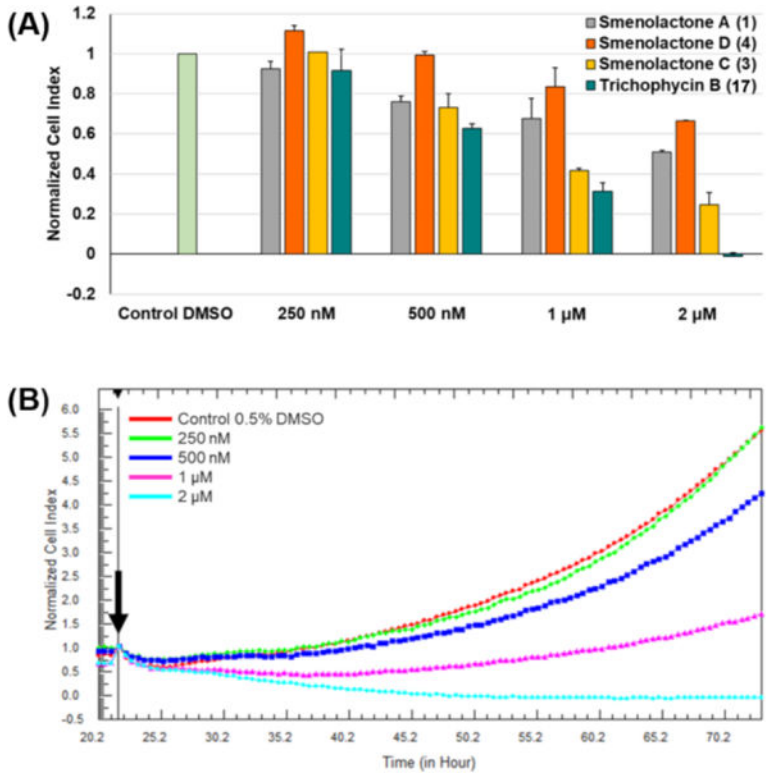

Figure 6.

Effects of smenolactones on the proliferation of MCF7 cells monitored in real time using the RTCA platform. (A) Normalized cell index (NCI) variation of the MCF7 cells exposed to different concentrations (250 nM, 500 nM, 1 µM, 2 µM) of trichophycin B and smenolactones A, C, and D after 48h of treatment. NCI values are relative to controls treated with DMSO vehicle. Data are presented as mean ± SD; n=3. $p < 0.0001$. (B) Normalized cell index kinetics of the MCF7 cells exposed to different concentrations (250 nM, 500 nM, 1 µM, 2 µM) of trichophycin B (**17**) and to DMSO vehicle. Arrow shows the starting point of treatment of the cells. Each cell index value was normalized to this starting point. Dose-dependent decrease of the slope of the NCI of MCF7 describes the steepness of cell proliferation curves after 48h treatment at each concentration.

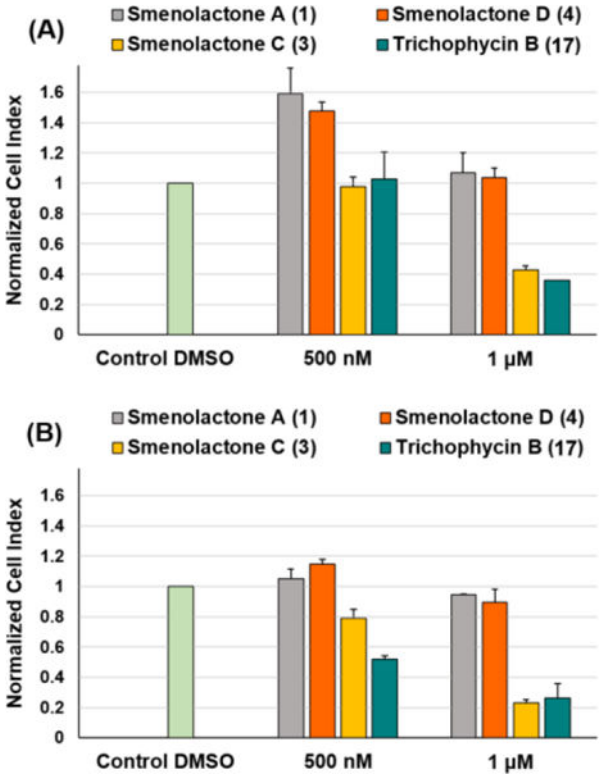

Figure 7.

Evaluation of antiproliferative effects of trichophycin B and smenolactones A, C, and D against PANC1 (A) and BxPC-3 (B) cell lines at 500 nM and 1 μM, within 48 h of treatment. NCI values are relative to controls treated with DMSO vehicle. Data are presented as mean ± SD; n=3. $p < 0.0001$.

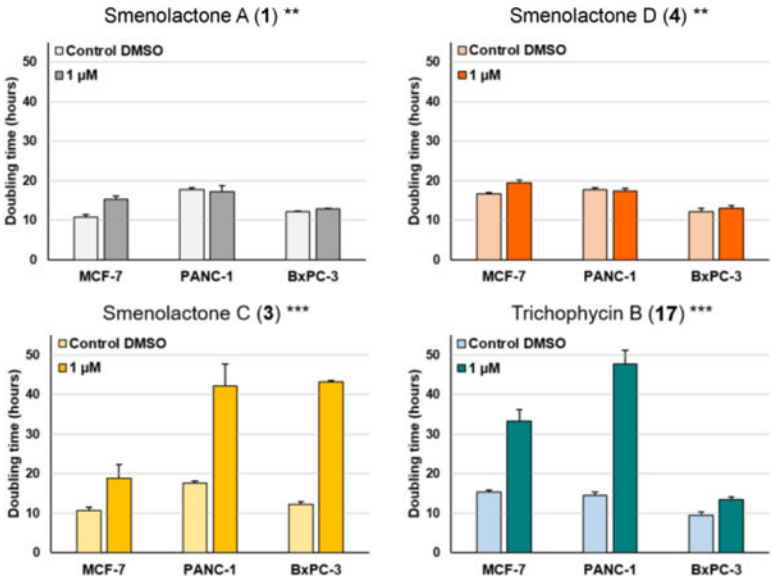

Figure 8.

Doubling times of NCI of MCF7, PANC-1 and BxPC-3 cancer cells after 48 h treatment with 1 μM of trichophycin B, smenolactones A, C, and D, and 0.5% DMSO. Doubling time is the time required for a curve cell index value to double. Data are presented as mean ± SD; n=3. ** $p < 0.001$; *** $p < 0.0001$.

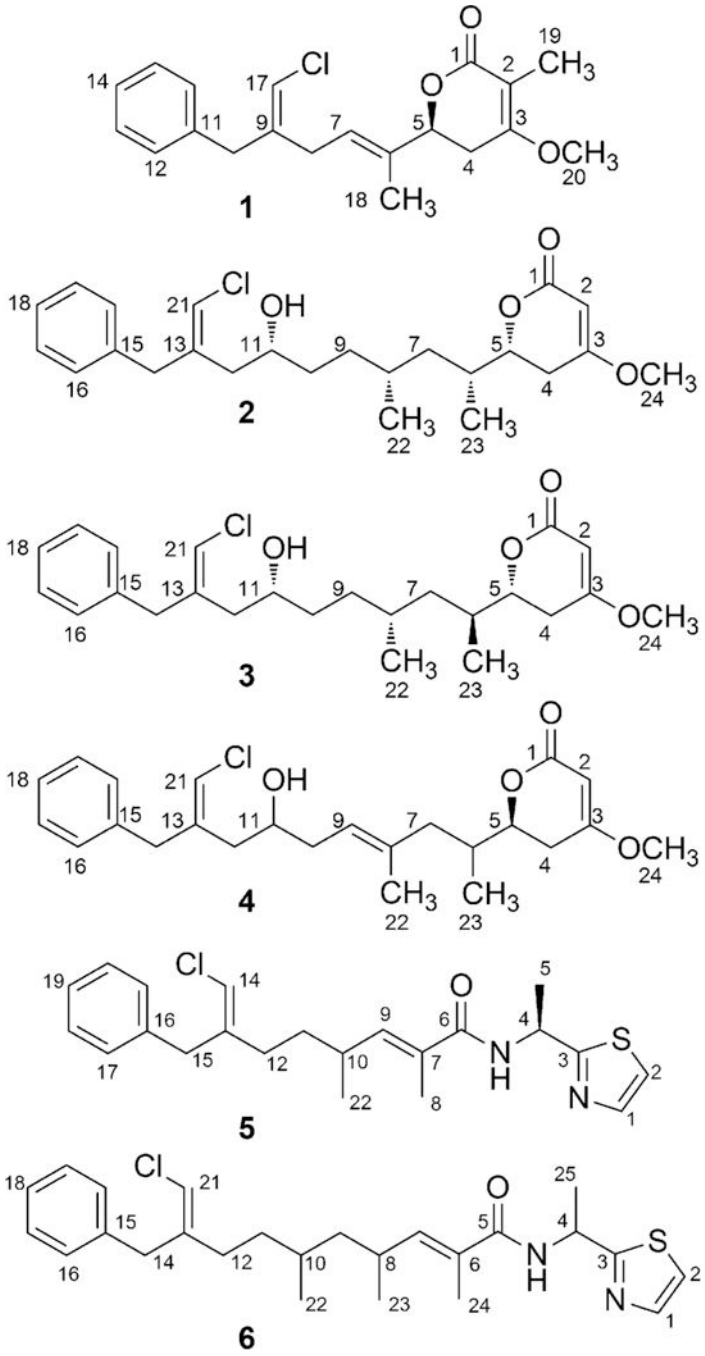

Chart 1.

Structures of the new chlorinated polyketides, smenolactones A (**1**), B (**2**), C (**3**), and D (**4**) isolated from *Smenospongia aurea* and of the new isoconulothiazole B (**5**) and conulothiazole C (**6**) isolated from *Trichodesmium* sp.

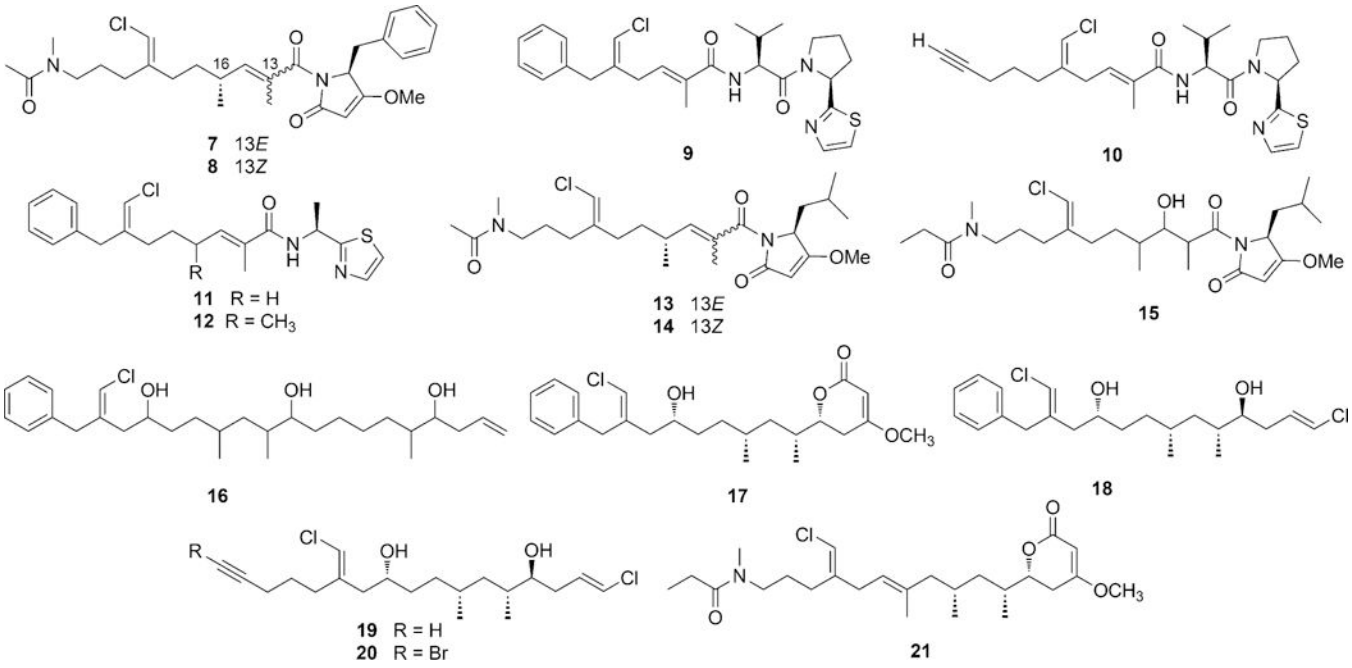

Chart 2.

Structures of smenamides A (**7**) and B (**8**), smenothiazoles A (**9**) and B (**10**) and conulothiazoles A (**11**) and B (**12**) isolated from *Smenospongia* spp, and of smenamides C (**13**), D (**14**), and E (**15**) and trichophycins A-F (**16–21**) isolated from *Trichodesmium sp.*

Table 1.

NMR data for trichophycin B (**17**) and smenolactones B-D (**2-4**) (CD_3OD, 700 MHz)

	trichophycin B (17)		smenolactone B (2)		smenolactone C (3)		smenolactone D (4)	
Pos.	**δ_C, type**	**δ_H, mult (*J* in Hz)**	**δ_C, type**	**δ_H, mult (*J* in Hz)**	**δ_C, type**	**δ_H, mult (*J* in Hz)**	**δ_C, type**	**δ_H, mult (*J* in Hz)**
1	170.9, C	-	170.9, C	-	170.9, C	-	170.9, C	-
2	90.3, CH	5.18, d (1.6)	90.2, CH	5.18, d (1.6)	90.1, CH	5.18, d (1.6)	90.2, CH	5.19, d (1.6)
3	176.8, C	-	176.6, C	-	176.7, C	-	176.5, C	-
4a	31.2, CH_2	2.65, ddd (17.2, 13.0, 1.7)	31.2, CH_2	2.66, ddd (17.1, 13.0, 1.8)	30.7, CH_2	2.62, ddd (17.2, 12.9, 1.6)	31.3, CH_2	2.68, ddd (17.2, 13.2, 1.7)
4b		2.32, br. dd (17.1, 3.6)		2.33, br. d (17.1, 3.6)		2.34, br. dd (17.2, 3.7)		2.30, br. dd (17.2, 3.5)
5	81.1, CH	4.32, ddd (13.1, 4.0, 4.0)	81.1, CH	4.33, ddd (12.8, 4.0, 4.0)	82.2, CH	4.26, ddd (12.8, 5.8, 3.7)	80.4, CH	4.35, ddd (13.1, 3.7, 3.7)
6	35.1, CH	1.85	35.2, CH	1.88, m	35.4, CH	1.94, ddq (12.1, 6.8, 3.7)	35.4, CH	1.93, m
7a	41.0, CH_2	1.43, ddd (13.4, 8.0, 5.5)	41.1, CH_2	1.47, ddd (13.5, 8.7, 6.2)	40.5, CH_2	1.37, ddd (13.3, 10.3, 3.7)	44.0, CH_2	2.25, m
7b		1.08, ddd (13.4, 8.6, 6.1)		1.11, ddd (13.5, 7.8, 5.5)		1.18, ddd (13.3, 10.3, 4.0)		1.93, m
8	30.9, CH	1.49, m	30.9, CH	1.54, m	31.1, CH	1.51, ddd (6.6, 3.7, 3.7)	136.2, C	
9a	32.9, CH_2	1.27, m	33.0, CH_2	1.37, m	35.2, CH_2	1.36, ddd (13.6, 12.7, 6.6)	124.3, CH	5.25, br. t (7.0)
9b		1.15, m		1.23, m		1.27, m		
10a	35.2, CH2	1.37, ddd (13.3, 10.3, 3.7)	35.2, CH_2	1.44, ddd (11.7, 9.8, 4.6)	35.8, CH_2	1.46, m	37.2, CH_2	2.19, m
10b		1.31, m		1.41, m				
11	70.3, CH	3.60, tt (7.5, 5.4)	70.8, CH	3.75, m	71.0, CH	3.76, ddd (12.7, 7.8, 4.4)	71.1, CH	3.84, m
12a	43.1, CH2	2.10, ddd (14.3, 4.9, 1.2)	38.9, CH_2	2.34, br. dd (13.3, 5.8)	38.9, CH_2	2.34, br. dd (13.5, 5.7)	38.1, CH_2	2.33, m
12b		2.09, ddd (14.3, 7.9, 1.2)		2.24, br. dd (13.3, 7.6)		2.24, br. dd (13.5, 7.8)		2.22, m
13	141.7, C		141.5, C	-	141.7, C	-	142.1, C	
14a	37.0, CH_2	3.73, br. d (14.5)	42.8, CH_2	3.48, br. s	42.8, CH_2	3.48, br. s	42.6, CH_2	3.48, br. s
14b		3.54, br. d (14.5)						
15	140.5, C		139.8, C	-	140.0, C	-	140.0, C	
16/20	130.1, CH	7.21, br. d (7.6)	130.0, CH	7.19, br. d (7.6)	130.0, CH	7.19, br. d (7.4)	130.1, CH	7.18, br. d (7.6)
17/19	129.7, CH	7.27, br. t (7.6)	129.4, CH	7.29, br. t (7.6)	129.5, CH	7.29, br. t (7.4)	129.5, CH	7.29, br. t (7.6)
18	127.4, CH	7.19, br. t (7.6)	127.5, CH	7.20, br. t (7.6)	127.5, CH	7.21, br. t (7.4)	127.7, CH	7.20, br. t (7.6)
21	115.8, CH	6.11, br. s	116.4, CH	6.05, br. s	116.4, CH	6.06, br. s	116.2, CH	6.04, br. s
22	20.7, CH_3	0.87, d (6.6)	20.7, CH_3	0.90, d (6.6)	19.6, CH_3	0.87, d (6.6)	16.1, CH_3	1.61, br. s

	trichophycin B (17)		smenolactone B (2)		smenolactone C (3)		smenolactone D (4)	
Pos.	**δ_C, type**	**δ_H, mult (*J* in Hz)**	**δ_C, type**	**δ_H, mult (*J* in Hz)**	**δ_C, type**	**δ_H, mult (*J* in Hz)**	**δ_C, type**	**δ_H, mult (*J* in Hz)**
23	15.2, CH_3	0.98, d (6.8)	15.2, CH_3	1.00, d (6.8)	15.1, CH_3	0.96, d (6.8)	14.9, CH_3	0.92, d (6.8)
24	57.0, CH_3	3.80, s	57.1, CH_3	3.80, s	57.1, CH_3	3.80, s	57.4, CH_3	3.80, s